European Spine Journal (2025) 34:3294–3303
https://doi.org/10.1007/s00586-025-08997-5

RESEARCH

Endplate preparation for anterior cervical discectomy and fusion: does the amount of endplate removed affect cage subsidence risk?

Alick P. Wang[1,2] · Thomas D. Slater[1] · Kay A. Raftery[1] · Spyros D. Masouros[1] · Hannah A. Levy[3] · Brett A. Freedman[3] · Nicolas Newell[1]

Received: 25 March 2025 / Revised: 12 May 2025 / Accepted: 24 May 2025 / Published online: 7 June 2025

Abstract

Purpose Subsidence after anterior cervical discectomy and fusion (ACDF) is a common complication that may be influenced by the degree of endplate removal prior to cage insertion. The optimal degree of endplate removal remains unclear; therefore, we performed a series of ex vivo experiments to elucidate the relationship between the aggressiveness of endplate preparation and subsidence risk.

Methods Human cadaveric subaxial cervical endplates were partially decorticated either conservatively ($n = 10$) or aggressively ($n = 9$). The degree of endplate removal was quantified using microCT. Subsidence was modelled by measuring the strength and stiffness of each specimen when an interbody cage was axially compressed into the endplate.

Results Conservative endplate preparation resulted in less endplate removal than aggressive endplate preparation (mass: 150 vs. 301 mg, $p < 0.001$; volume: 47 vs. 88mm^3, $p = 0.01$; thickness: 0.02 vs. 0.16 mm, $p = 0.004$). There was no significant difference between the two groups with respect to endplate strength (2.04 vs. 2.04kN, $p = 0.99$) or stiffness (2.38 vs. 2.41kN/mm, $p = 0.89$). Bone mineral density (BMD) was similar between the two groups (271.6 vs. 271.9 mg/cm^3, $p = 0.98$) but positively correlated with endplate strength (effect size 0.68, $p = 0.001$).

Conclusions When performing partial cervical endplate decortication, the degree of bony endplate removal did not significantly predict endplate integrity during ex vivo compression testing, but greater BMD was associated with increased strength. The degree of endplate removal should be based on individual patient factors and intraoperative findings to achieve the ideal cage-endplate interface.

Keywords Interbody fusion · Cage subsidence · Endplate preparation

Introduction

Anterior cervical discectomy and fusion (ACDF) is a commonly performed surgical treatment for disc herniations, spinal stenosis, and spine fractures. Although techniques and implant technology have continued to evolve since ACDF was first described in the 1950s, the basic premise remains unchanged: removing a portion of the intervertebral disc and replacing it with a graft that promotes fusion of the two adjacent vertebral bodies [1].

✉ Alick P. Wang
alickwang@gmail.com

✉ Nicolas Newell
n.newell09@imperial.ac.uk

Thomas D. Slater
t.slater22@imperial.ac.uk

Kay A. Raftery
kay.raftery18@imperial.ac.uk

Spyros D. Masouros
s.masouros04@imperial.ac.uk

Hannah A. Levy
hannahlevy2121@gmail.com

Brett A. Freedman
Freedman.Brett@mayo.edu

1 Department of Bioengineering, Imperial College London, London, UK

2 Division of Neurosurgery, Department of Surgery, University of Ottawa, Ottawa, Canada

3 Department of Orthopedic Surgery, Mayo Clinic, Rochester, USA

Subsidence, the migration of the cage into the vertebral body endplate, occurs in approximately 21% of cases [2]. Subsidence can lead to spinal malalignment and deformity, pain, neurological injury, or pseudo-arthrosis [2]. Factors believed to increase its risk include patient factors such as age [3], smoking [4], and osteoporosis [5] as well as intra-operative factors such as decreased cage width [6], increased cage height, over-distraction of the endplates [7], stiffer cage material [8], suboptimal cage position [9], lack of instrumented fixation [10], and over-preparation of the endplate [10–12].

Every interbody fusion involves endplate preparation prior to implant insertion, but there is variation in the technique for and degree of endplate removal. On one hand, insufficient preparation (leaving behind portions of disc material or cartilaginous endplate) may prevent fusion [13] as decortication exposes the vascular supply and stem cells from the trabecular bone and marrow [14]. On the other hand, over-zealous preparation may increase the risk of subsidence [10–12] by reducing the ability of the vertebral body to withstand compressive axial loads [15].

However, the optimal proportion of endplate removal remains unknown. In addition, it is not known whether there is a threshold of bony endplate removal beyond which the risk of subsidence increases or whether additional endplate removal increases subsidence continuously. In this study, we investigated the relationship between bony endplate removal and the risk of cage subsidence through biomechanical experiments performed on human cadaveric cervical spine specimens.

Methods

Specimens

Four cadaveric cervical spines were obtained from human donors aged 22–58 years (mean 45.5 years). Ethical approval was obtained from [Blinded for Review]. Each spine was imaged with computed tomography (SOMATOM, Siemens AG, Munich, Germany) using a clinical spine protocol (field of view: 35.8 cm, 120 kV; matrix: 512 × 512; slice thickness: 1 mm) to allow specimens with prior cervical spine surgery, osteoporosis (BMD < 80 mg/cm^3) [16], extensive degenerative changes, fractures, and lytic or blastic defects to be excluded. The specimens were frozen at -20 °C until dissection.

Dissection

Twenty subaxial (C3–7) vertebral bodies were dissected. Surrounding soft tissues were discarded. The pedicles, transverse processes, facets, laminae, and spinous processes were removed, leaving the vertebral bodies and endplates intact. The inferior endplates were shallowly embedded in polymethylmethacrylate (PMMA) bone cement such that the superior endplate was parallel to the horizontal plane.

Endplate APD (anteroposterior diameter of superior endplate) as well as vertebral body height (mid-sagittal cranio-caudal length) were measured using callipers to calculate relative proportions of endplate removed (Table 1).

Imaging

MicroCT (Zeiss Xradia Versa, Pleasanton, California, USA) of the specimens were acquired at 80 kV, 7 W, 0.4x objective, LE5 (low energy) filter with 1s exposure and 801 images per scan (50.7 µm resolution). Calibration was performed using a MicroCT-HA D4.5 phantom (QRM GmbH, Möhrendorf, Germany) with hydroxyapatite concentrations of 0, 50, 200, 800, and 1200 mg/cm^3. Bone mineral density (BMD) was calculated by measuring trabecular density in Hounsfield units (HU) at three separate axial planes within each vertebra [17]. Measurements were taken using 3D Slicer (Brigham and Women's Hospital, Boston, USA). Volumes were segmented using a density cut-off to exclude soft tissue and include cortical and trabecular bone. Cortical endplate thickness was determined using an average of several (3 × 3) measurements per vertebra [12].

Table 1 Baseline characteristics of specimens prior to testing (BMD: bone mineral density; APD: anteroposterior diameter)

	Aggressive		Conservative		
	Mean	SD	Mean	SD	*p*-value
Cadaver characteristics					
Age (years)	46.9	14.5	43.9	15.4	0.66
Height (cm)	177.8	4.9	176.5	4.8	0.76
Weight (kg)	75.9	7.9	73.7	6.9	0.55
Vertebra characteristics					
BMD (mg/cm^3)	271.6	41.3	271.9	41.9	0.98
Endplate APD (mm)	16.9	2.2	16.7	1.9	0.80
Vertebral height (mm)	12.7	0.8	12.3	1.0	0.43
Endplate thickness (mm)	0.59	0.3	0.48	0.1	0.33

Table 2 Quantification of endplate removal and biomechanical properties

	Aggressive		Conservative		
	Mean	SD	Mean	SD	*p*-value
Endplate preparation					
Mass removed (mg)	301	67	150	37	**< 0.001**
Proportion of mass removed (%)	3.4%	0.4%	1.7%	0.5%	**< 0.001**
Volume removed (mm^3)	88	39	47	26	**0.01**
Proportion of volume removed (%)	2.9%	0.8%	1.5%	0.8%	**0.002**
Thickness removed (mm)	0.16	0.11	0.02	0.02	**0.004**
Thickness remaining (mm)	0.43	0.25	0.46	0.15	0.76
Proportion of thickness removed (%)	28%	14%	4%	3%	**< 0.001**
Trabecular bone exposed (n, %)	0/10 (0%)		6/9 (67%)		**< 0.001**
Biomechanical properties					
Stiffness (kN/mm)	2.41	0.4	2.38	0.7	0.89
Displacement (mm)	1.9	0.5	2.0	0.5	0.73
Ultimate strength (kN)	2.04	0.5	2.04	0.5	0.99
Fracture size (mm)	1.2	0.4	1.3	0.3	0.38

Test groups

The endplates were divided into two groups: "conservative" ($n = 10$) and "aggressive" endplate preparation ($n = 10$). Means and standard deviations of vertebral dimensions, BMD, age, and vertebral level were calculated to ensure similar distributions within the two groups (Table 2). Specimens from each cadaver were distributed equally between the groups.

Endplate preparation

Endplate preparations were performed by a single surgeon to improve reproducibility. In both conservative and aggressive groups, endplate preparation began by removal of all disc material and cartilaginous endplate using a scalpel and periosteal elevator to expose a denuded bony endplate.

In the conservative group, we performed the minimal amount of decortication required to achieve a flat contact surface for the cage – this typically involved shaving the periphery of the endplate due to its curvature. This was done using a high-speed drill (30,000 rpm). Care was taken to not expose any underlying trabecular bone.

In the aggressive group, the drill was used to decorticate the entire endplate, ensuring that a thin layer of bone was removed throughout. Further decortication was then performed wherever necessary to produce a flat contact for the cage. Exposure of the trabecular bone in certain areas was permitted but not required.

Specimens were re-imaged with microCT. Pre- and post-preparation endplate volume and thickness were calculated. Pre-and post-preparation vertebral mass was measured using a scale (0.01 g resolution). Endplates were also classified as either having trabecular bone exposed or not (Table 2).

Cage design

A custom interbody cage was modelled in Fusion 360 (Autodesk, Inc., San Francisco, California, USA) and 3D-printed (Fig. 1a) using micro-carbon-fibre-filled nylon (Onyx, Markforged, Waltham, Massachusetts, USA); see Supplementary File 1 for cage design. The cage was 14 mm (lateral) by 12 mm (anteroposterior) by 6 mm (craniocaudal).

Compression test

Each specimen was thawed to room temperature (20 °C) and tested sequentially. The specimens were placed in an Instron 5866 Universal Testing Machine (Norwood, Massachusetts, USA) using a 10kN load cell (Fig. 1b). The specimens were clamped to prevent horizontal translation. A new cage was

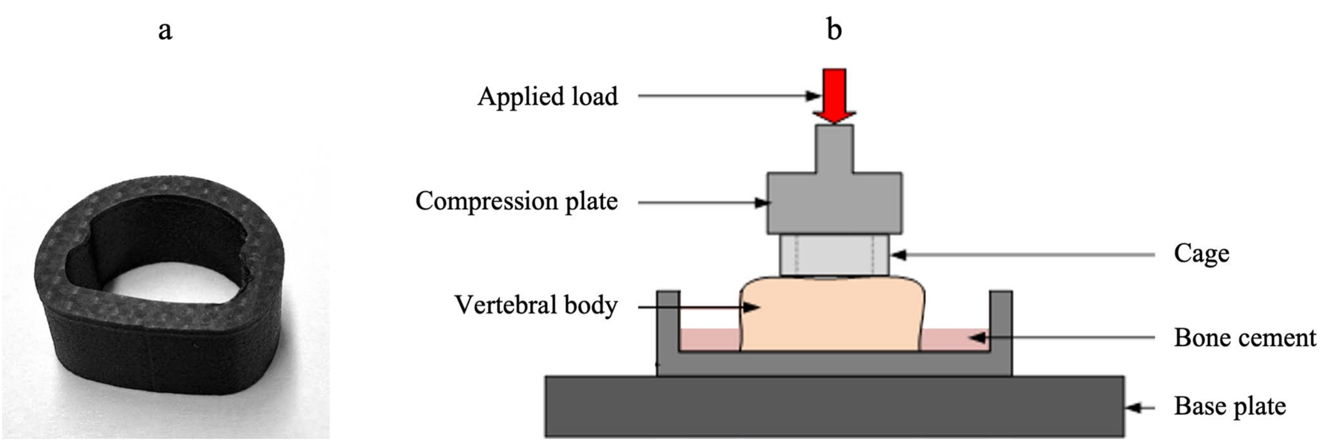

Fig. 1 **a**: 3D-printed interbody cage (micro-carbon-fibre-filled nylon). **b**: Experimental setup for compression testing – a compressive load was applied to the cage, which was placed on top of the endplate; the vertebral body was potted in PMMA bone cement

placed on top of each endplate with the anterior margin of the cage flush with the anterior margin of the vertebral body (ring apophysis).

A compressive preload of 50 N was initially applied to ensure full contact between the compression platen and the cage (Fig. 1b). Force and displacement were then recorded while ramp compression was applied at 10 mm/min. The first specimen (aggressive group) was discarded prior to statistical analysis due to a technical error during compression. A total of 19 specimens (10 conservative, 9 aggressive) were analysed.

Failure was defined as a decrease in compressive force [15] (≥3% from peak) or ≥3 mm displacement [2, 18]. Compliance in the cage was accounted for through a compression test on an isolated cage (up to a maximum force of 8kN); displacement values from test were subtracted from specimen displacements such that only displacement due to endplate subsidence were included in the final force-displacement curves (Fig. 2).

Quantification of trabecular microarchitecture

Specimens were re-imaged with microCT. Endplate volume and thickness were re-measured. Endplate "fracture size" was defined and measured as the distance from the surface of the endplate to the line beyond which the bone appeared structurally intact.

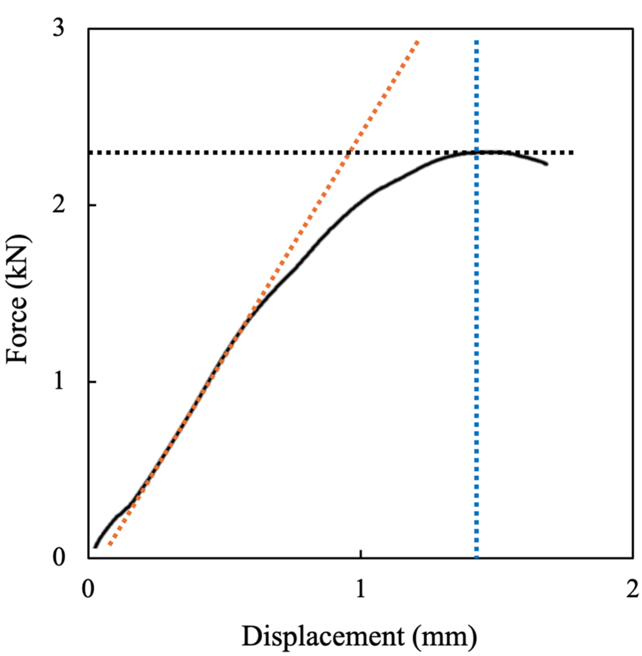

Fig. 2 Typical force-displacement curve (solid black line) for one of the specimens obtained from compression testing. The dotted black line represents ultimate strength (2.3kN for this specimen) and the dotted orange line represents the linear region stiffness (2.5kN/mm for this specimen). The dotted blue line represents the displacement at peak force (1.4 mm for this specimen)

All microarchitecture parameters were calculated using ImageJ (v1.53t, Bethesda, Maryland, US) and the BoneJ plugin (Doube et al., 2010). The micro-CT image of each cervical vertebra was thresholded at the second local trough of the histogram. To exclude the cortical endplate, a 5 mm thick region of interest (ROI) was isolated where the most superior slice was 2 mm below the slice in which the superior endplate was continuous in the axial plane. The ROI was further manually segmented to exclude the peripheral cortical bone.

Statistical analysis

Statistics were performed using Microsoft Excel (Redmond, Washington, USA) and Prism (v10.0.2, GraphPad Software, San Diego, California, United States). For two-group comparisons, Shapiro-Wilk and Brown-Forsythe tests were used to assess normality and heteroscedasticity, respectively. Unpaired two-tailed Student's t-tests were performed, or Mann-Whitney where normality was violated. Welch's t-test was used in the case of unequal variances. Linear associations between two variables were analysed using Pearson's correlation coefficient. Post-hoc power analyses were performed in G*Power [19]. An alpha <0.05 was considered significant.

Results

Baseline specimen characteristics

Cadaver (age, height, weight) and vertebral (cervical level, BMD, dimensions) characteristics for the aggressive and conservative groups are presented in Table 1. There were no significant differences with respect to potential confounders such as age, BMD, and vertebral level.

Quantification of endplate removal

Mean endplate thickness prior to preparation was 0.53 mm (range 0.26–1.27 mm). There was a significant difference in the endplate mass, thickness, and volume removed between the two preparation techniques (Table 2). Trabecular bone was exposed (breach of the bony endplate) in 6/9 (67%) of the aggressively prepared endplates, and 0/10 (none) of the conservatively prepared endplates ($p<0.001$). Figure 3 shows that the methods for quantifying endplate removal (mass, thickness, volume) correlated with each other ($p<0.001$).

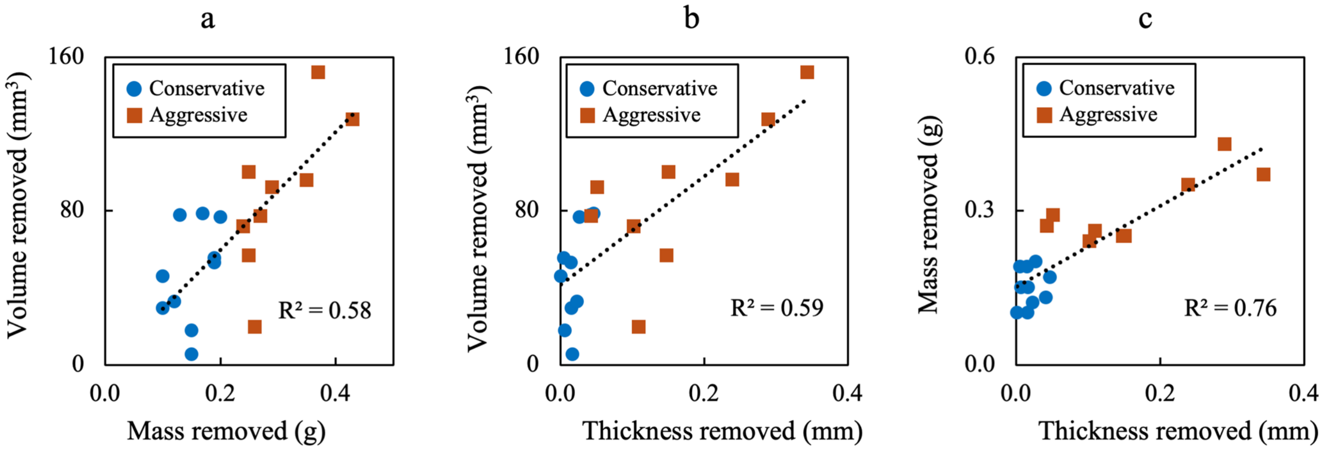

Fig. 3 Relationships between endplate mass, thickness, and volume demonstrating consistency between different methods of quantifying endplate removal (blue circles: conservative; orange squares: aggressive). **a**: Endplate mass removed plotted against volume removed, $p<0.001$. **b**: Endplate thickness removed plotted against volume removed, $p<0.001$. **c**: Endplate thickness removed plotted against mass removed, $p<0.001$

Compression testing

A typical force-displacement response of the cage being compressed into the endplate of one of the samples is shown in Fig. 2.

Stiffness values ranged from 1.6–3.6kN/mm, with a mean of 2.4kN/mm. Displacement values at peak force ranged from 1.2 to 2.6 mm, with a mean of 1.9 mm. Strength values ranged from 1.2–2.7kN, with a mean of 2.0kN. Fracture size ranged from 0.8 to 2.0 mm, with a mean of 1.2 mm. There were no statistically significant differences in average stiffness (kN/mm), final displacement (mm), or ultimate compressive strength (kN) between the aggressive and conservative groups (Table 2).

Higher BMD (mg/cm^3) was associated with greater endplate strength (kN), as seen in Fig. 4c ($p=0.001$, effect size $=0.68$). There was no relationship between BMD and stiffness (Fig. 4a), displacement (Fig. 4b), or fracture size (Fig. 4d).

No significant trend was observed between any biomechanical properties (strength, stiffness, displacement, fracture size) and the amount of endplate removed (proportion of mass removed (Fig. 5a), thickness of endplate removed (Fig. 5b), remaining endplate thickness (Fig. 5c), or volume of endplate removed (Fig. 5d)). There was no significant difference between the samples with breach of the trabecular bone vs. without breach with respect to strength (2.0 vs. 2.1kN, $p=0.77$) or stiffness (2.5 vs. 2.3kN/mm, $p=0.61$).

There was a significant correlation between trabecular thickness and stiffness ($p=0.02$, effect size $=0.53$) as well as strength ($p=0.03$, effect size $=0.49$) (Fig. 6a and b). There was no significant correlation between trabecular separation and stiffness ($p=0.67$) nor strength ($p=0.90$) (Fig. 6c and d).

Discussion

Our study is the first ex vivo biomechanical study to comprehensively investigate whether partial endplate decortication affects cage subsidence in the human cervical spine. Our data reveal the effects of partial endplate removal on endplate strength, stiffness, and fracture size.

Degree of partial endplate removal

We found that when the endplate is partially removed, the degree of endplate removal does not correlate with endplate integrity. The mean percentage of endplate thickness removed was 4% in the conservative group and 28% in the aggressive group (range 0.1–57.8%). Due to the natural endplate curvature, a mean removal of 28% in the aggressive group was already associated with cortical breach (exposure of trabecular bone) in the majority (6/9) of specimens. Had we performed even more aggressive decortication, we would have likely observed cortical breaches in all specimens. While this may have resulted in enough endplate removal to affect endplate strength or stiffness, our aim was to study the effects of partial, not complete, endplate removal. Previous investigators have already determined that vertebrae with complete endplate removal have significantly decreased load to failure than specimens with an intact endplate [12], but this situation does not reflect realistic endplate preparation conditions during ACDF.

Conservative vs. aggressive endplate decortication

There is disagreement amongst surgeons about the ideal technique for and amount of endplate removal. In addition, it has yet to be experimentally demonstrated that the

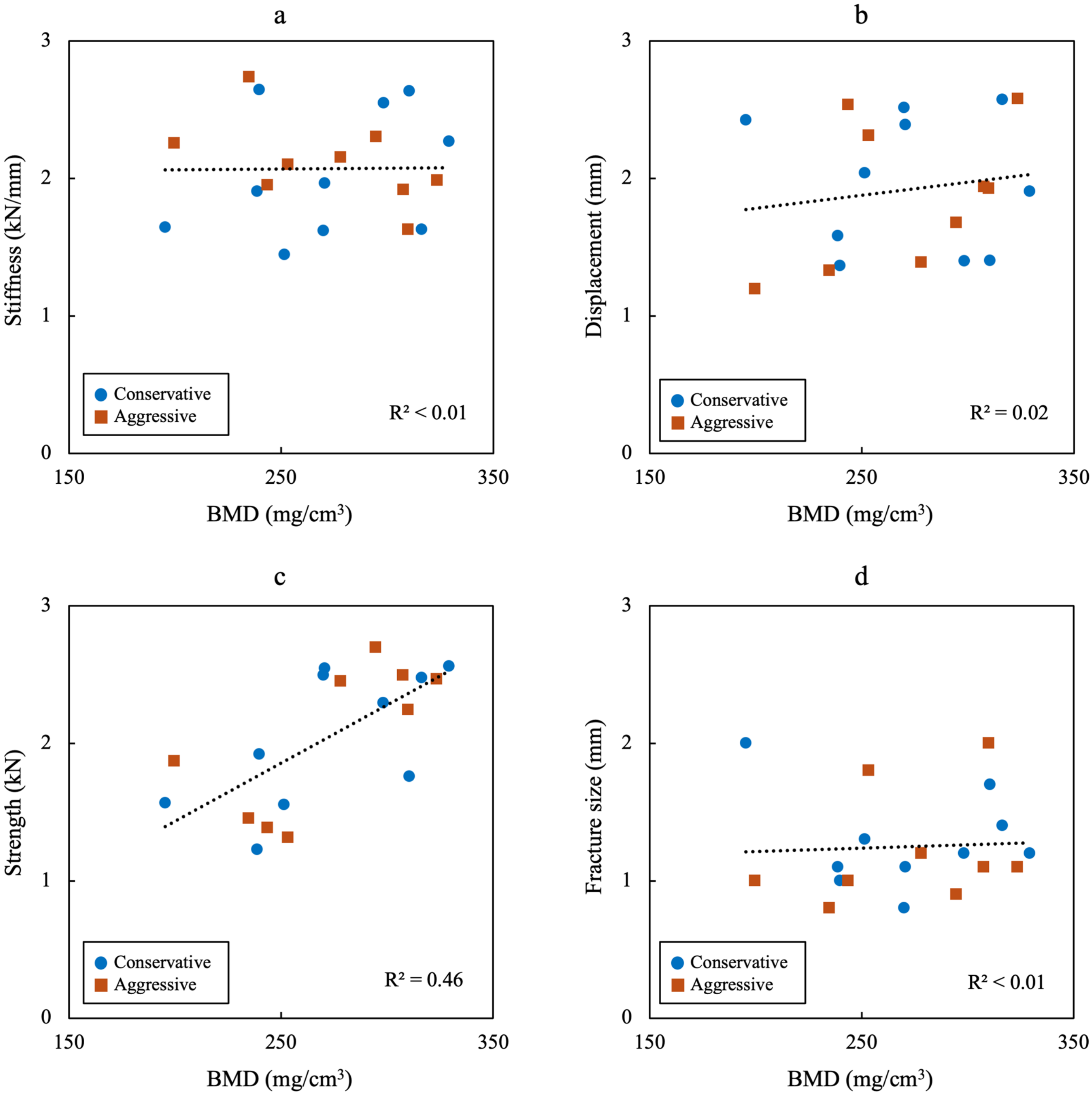

Fig. 4 Correlation between BMD and biomechanical properties (blue circles: conservative; orange squares: aggressive). **a**: BMD values plotted against the linear region stiffness (kN/mm) of each specimen, $p=0.97$. **b**: BMD values plotted against the displacement (mm) at maximum force of each specimen, $p=0.53$. **c**: BMD values plotted against the ultimate compressive strength (kN) of each specimen, $p=0.001$, effect size 0.68. **d**: BMD values plotted against the fracture size (mm) of each specimen, $p=0.83$

degree of endplate decortication can be deliberately varied in a realistic and reproducible fashion. Other ex vivo studies have used 1–2 mm indentation probes to model partial endplate destruction [20, 21], which does not replicate endplate preparation during ACDF. Our data demonstrate that an intentional modification of endplate preparation aggression does translate to a quantifiable and reproducible difference in endplate removal (Table 2).

Bone mineral density and trabecular architecture

Our study validates previous work by other authors that trabecular BMD is a significant predictor of the yield strength of specimens in compression testing [12, 21]. We found a clear correlation between BMD and ultimate strength ($p=0.001$), as shown in Fig. 4c.

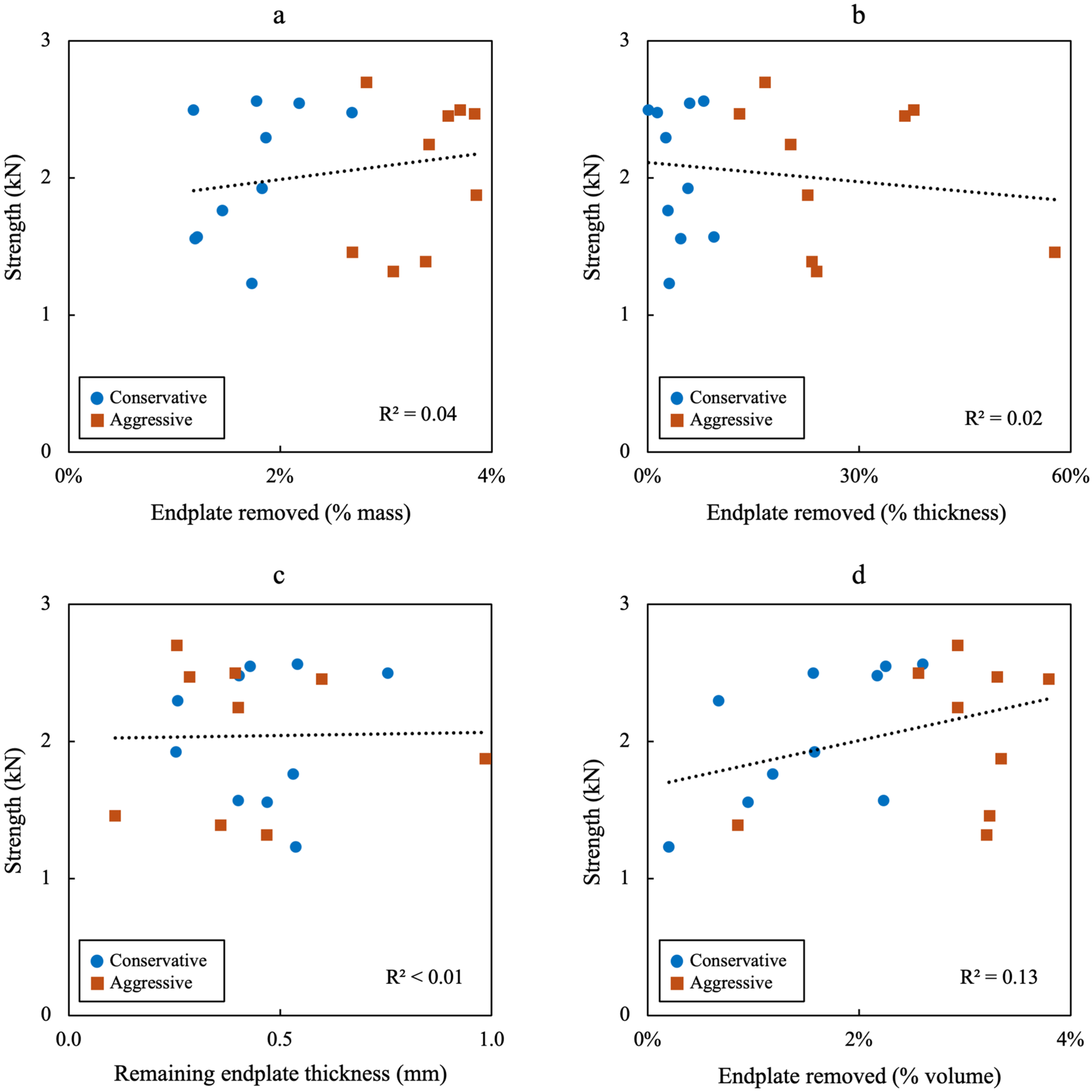

Fig. 5 Relationship between endplate preparation and biomechanical properties (blue circles: conservative; orange squares: aggressive). **a**: Proportion of mass removed plotted against ultimate compressive strength (kN), $p=0.43$. **b**: Proportion of endplate thickness removed plotted against strength (kN), $p=0.56$. **c**: Remaining endplate thickness removed plotted against strength (kN), $p=0.94$. **d**: Proportion of volume removed plotted against strength (kN), $p=0.14$

Trabecular thickness was significantly associated with both stiffness and strength (Fig. 6a and b). These data suggest that density of the trabecular bone (larger strut diameter) predicts subsidence and support a subsidence mechanism involving buckling of internal trabeculae. This is consistent with Palepu et al.'s observation that trabecular bone volume fraction was better than endplate thickness for predicting force to subsidence [22]. However, due to the smaller effect size likely generated from the small sample tested, these relationships must be treated with caution. Interestingly, trabecular separation was not correlated with either stiffness or strength (Fig. 6c and d). However, because cervical vertebrae exhibit significantly greater trabecular thickness than thoracic and lumbar vertebrae [23], relative thickness may be a greater determinant of strength in this region.

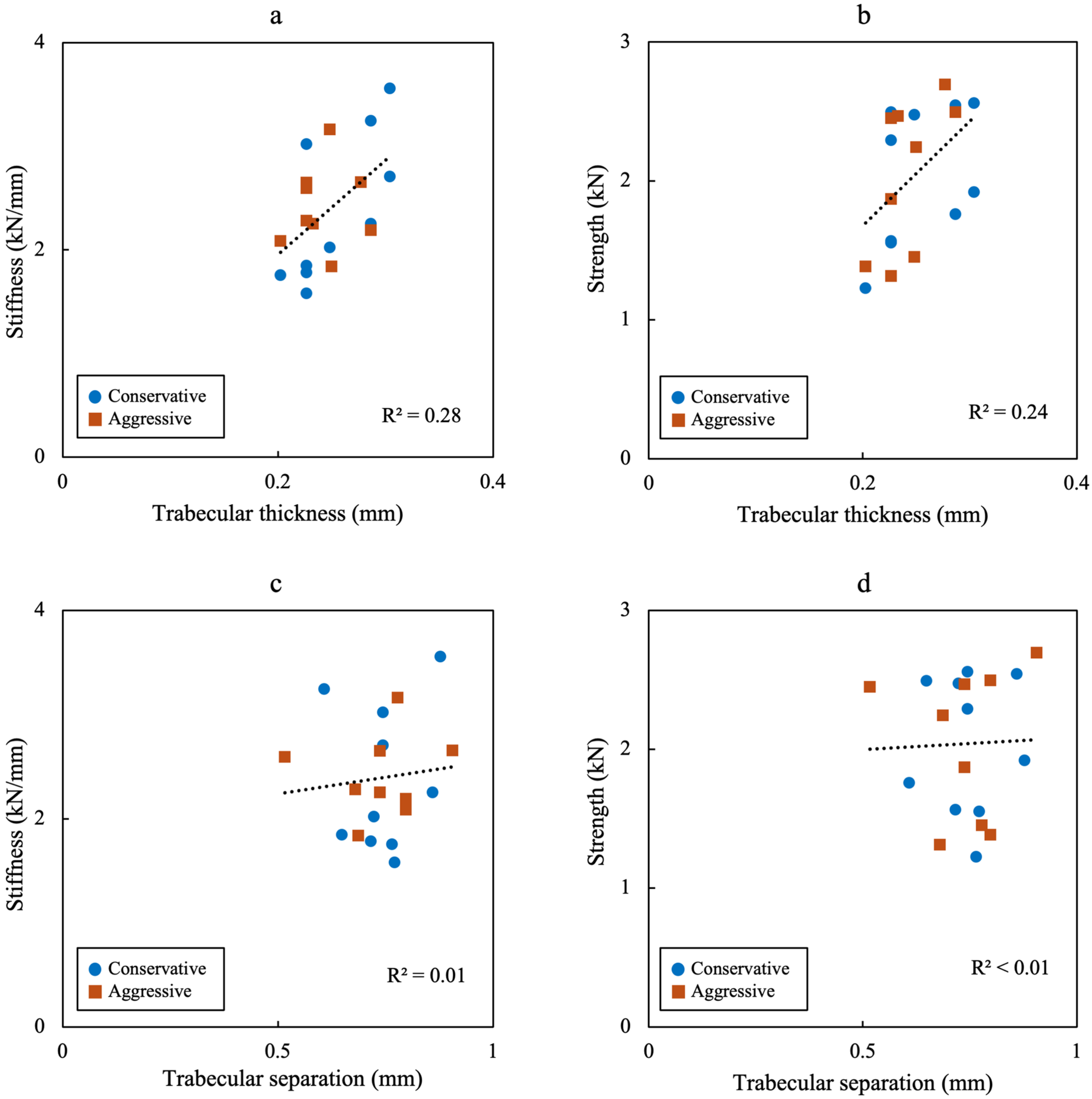

Fig. 6 Relationship between trabecular microarchitecture and biomechanical properties (blue circles: conservative; orange squares: aggressive). **a**: Median trabecular thickness plotted against stiffness (kN/mm), $p=0.02$, effect size 0.53. **b**: Median trabecular thickness plotted against ultimate compressive strength (kN), $p=0.03$, effect size 0.49. **c**: Median trabecular separation plotted against stiffness (kN/mm), $p=0.67$. **d**: Median trabecular separation plotted against strength (kN), $p=0.90$

Fracture size

MicroCT of post-compression specimens revealed that endplate fractures resulted from destruction of the trabecular bony architecture within a few millimetres of the endplate (endplate fracture size, Table 2), but the rest of the vertebral body, including much of the deeper trabecular bone structure, was largely maintained. In other words, the fracture occurred in the endplate itself and the trabecular bone close to the endplate, but not within the central trabecular bone of the vertebra. It is therefore interesting that BMD reliably predicts endplate integrity. Although we hypothesized that a greater BMD would predict a smaller fracture size, we did not observe any relationship between the two

($p = 0.83$). Our understanding of this phenomenon remains quite limited.

Limitations

In our study, we investigated only superior/cranial endplates, which is the site of most (67–89%) instances of subsidence [24]. However, in vivo cage subsidence is complex and involves two endplate-cage interfaces, with an interbody cage compressed between two endplates.

Additionally, our specimens included the entire subaxial spine (C3–7), which is representative of most clinical cases of ACDF. While studies have shown no significant difference in BMD between subaxial cervical levels [12], differences in physiological loading exist in vivo [25], which may limit the generalizability of our data. Our cadaveric specimens are from relatively young donors (mean age: 45.5 years) with relatively normal BMD; caution should be used in applying our findings to elderly or osteoporotic patients.

Finally, our biomechanical testing involved ramped pure axial compression. This is a common method for studying vertebral endplate subsidence [12, 20, 21] as its simplicity allows for reproducibility and comparison between studies; however, clinical cases of subsidence may be a result of more complex cyclic loading with greater degrees of freedom, including flexion/extension, lateral bending, and axial rotation.

Conclusions

We performed ex vivo biomechanical experiments to elucidate the relationship between the degree of endplate preparation and subsidence risk in ACDF. We demonstrated that endplates can be reproducibly decorticated in a conservative or aggressive fashion and that endplate preparation can be quantified using mass, thickness, or 3D volume. When performing partial endplate decortication, the degree of bony endplate removal did not significantly predict the ultimate compressive strength or stiffness of endplates during axial compression testing with an interbody cage, while increased BMD was associated with greater strength. The degree of endplate removal should therefore be left to surgeon discretion, considering individual patient factors and intraoperative findings to achieve the ideal cage-endplate interface.

Supplementary Information The online version contains supplementary material available at https://doi.org/10.1007/s00586-025-08997-5.

Acknowledgements We would like to thank Andra Topan for her help with the cadaveric specimens, Niraj Kanabar for 3D printing the cages, and John R Waldock for his help with machining PEEK cage prototypes. Human samples used in this research project were obtained from the Imperial College Healthcare Tissue and Biobank (ICHTB). ICHTB is supported by the National Institute for Health Research (NIHR) Biomedical Research Centre based at Imperial College Healthcare NHS Trust and Imperial College London. ICHTB is approved by Wales REC3 to release human material for research (22/WA/0214), and the samples for this project (R23040) were issued from sub-collection reference number BIO_SM_14_034.

Author contributions APW and NN conceived the study design and methodology. APW, TS, and KR performed the experiments. APW and KR analysed the data. APW and NN prepared the figures. SM obtained the specimens. NN obtained grant funding. BAF, SM, and NN were responsible for study overview. APW, TS, KR, and NN wrote the main manuscript text. All authors reviewed and edited the manuscript.

Data availability No datasets were generated or analysed during the current study.

Declarations

Competing interests The authors declare no competing interests.

References

1. Cloward RB (1958) The anterior approach for removal of ruptured cervical disks. J Neurosurg 15:602–617. https://doi.org/10.3171/jns.1958.15.6.0602
2. Noordhoek I, Koning MT, Jacobs WCH, Vleggeert-Lankamp CLA (2018) Incidence and clinical relevance of cage subsidence in anterior cervical discectomy and fusion: a systematic review. Acta Neurochir (Wien) 160:873–880. https://doi.org/10.1007/s00701-018-3490-3
3. Lee Y-S, Kim Y-B, Park S-W (2014) Risk factors for postoperative subsidence of Single-Level anterior cervical discectomy and fusion: the significance of the preoperative cervical alignment. Spine 39:1280. https://doi.org/10.1097/BRS.0000000000000400
4. Bartels RHMA, Donk RD, Feuth T (2006) Subsidence of standalone cervical carbon fiber cages. Neurosurgery 58:502–508 discussion 502–508. https://doi.org/10.1227/01.NEU.0000197258.30821.50
5. Oh KW, Lee JH, Lee J-H et al (2017) The correlation between cage subsidence, bone mineral density, and clinical results in posterior lumbar interbody fusion. Clin Spine Surg 30:E683–E689. https://doi.org/10.1097/BSD.0000000000000315
6. Marchi L, Abdala N, Oliveira L et al (2013) Radiographic and clinical evaluation of cage subsidence after stand-alone lateral interbody fusion: clinical Article. SPI 19:110–118. https://doi.org/10.3171/2013.4.SPINE12319

7. Igarashi H, Hoshino M, Omori K et al (2019) Factors influencing interbody cage subsidence following anterior cervical discectomy and fusion. Clin Spine Surg 32:297. https://doi.org/10.1097/BSD.0000000000000843
8. Chong E, Pelletier MH, Mobbs RJ, Walsh WR (2015) The design evolution of interbody cages in anterior cervical discectomy and fusion: a systematic review. BMC Musculoskelet Disord 16:99. https://doi.org/10.1186/s12891-015-0546-x
9. Briski DC, Goel VK, Waddell BS et al (2017) Does spanning a lateral lumbar interbody cage across the vertebral ring apophysis increase loads required for failure and mitigate endplate violation. Spine 42:E1158–E1164. https://doi.org/10.1097/BRS.0000000000002158
10. Pinder EM, Sharp DJ (2016) Cage subsidence after anterior cervical discectomy and fusion using a cage alone or combined with anterior plate fixation. J Orthop Surg (Hong Kong) 24:97–100. https://doi.org/10.1177/230949901602400122
11. Lin M, Paul R, Shapiro SZ et al (2022) Biomechanical study of cervical endplate removal on subsidence and migration in multilevel anterior cervical discectomy and fusion. Asian Spine J 16:615–624. https://doi.org/10.31616/asj.2021.0424
12. Lim TH, Kwon H, Jeon CH et al (2001) Effect of endplate conditions and bone mineral density on the compressive strength of the graft-endplate interface in anterior cervical spine fusion. Spine (Phila Pa 1976) 26:951–956. https://doi.org/10.1097/00007632-200104150-00021
13. Li H, Zou X, Laursen M et al (2002) The influence of intervertebral disc tissue on anterior spinal interbody fusion: an experimental study on pigs. Eur Spine J 11:476–481. https://doi.org/10.1007/s00586-002-0455-1
14. Slappey G, Toribatake Y, Ganey TM et al (1998) Guidelines to decortication in posterolateral spine fusion. J Spinal Disord 11:102–109
15. Hou Y, Yuan W, Kang J, Liu Y (2013) Influences of endplate removal and bone mineral density on the Biomechanical properties of lumbar spine. PLoS ONE 8:e76843. https://doi.org/10.1371/journal.pone.0076843
16. The American College of Radiology (2023) ACR–SPR–SSR practice guideline for the performance of quantitative computed tomography (QCT) bone densitometry. Revised 2023 (Resolution 15).
17. Schreiber JJ, Anderson PA, Hsu WK (2014) Use of computed tomography for assessing bone mineral density. FOC 37:E4. https://doi.org/10.3171/2014.5.FOCUS1483
18. Kao T-H, Wu C-H, Chou Y-C et al (2014) Risk factors for subsidence in anterior cervical fusion with stand-alone polyetheretherketone (PEEK) cages: a review of 82 cases and 182 levels. Arch Orthop Trauma Surg 134:1343–1351. https://doi.org/10.1007/s00402-014-2047-z
19. Faul F, Erdfelder E, Lang A-G, Buchner A (2007) G*Power 3: a flexible statistical power analysis program for the social, behavioral, and biomedical sciences. Behav Res Methods 39:175–191. https://doi.org/10.3758/bf03193146
20. Cheng C-C, Ordway NR, Zhang X et al (2007) Loss of cervical endplate integrity following minimal surface Preparation. Spine 32:1852–1855. https://doi.org/10.1097/BRS.0b013e31811ece5a
21. Ordway NR, Lu Y-M, Zhang X et al (2007) Correlation of cervical endplate strength with CT measured subchondral bone density. Eur Spine J 16:2104–2109. https://doi.org/10.1007/s00586-007-0482-z
22. Palepu V, Helgeson MD, Molyneaux-Francis M, Nagaraja S (2019) The effects of bone microstructure on subsidence risk for ALIF, LLIF, PLIF, and TLIF spine cages. J Biomech Eng 141. https://doi.org/10.1115/1.4042181
23. Schröder G, Jabke B, Schulze M et al (2021) A comparison, using X-ray micro-computed tomography, of the architecture of cancellous bone from the cervical, thoracic and lumbar spine using 240 vertebral bodies from 10 body donors. Anat Cell Biology 54:25–34. https://doi.org/10.5115/acb.20.269
24. Barsa P, Suchomel P (2007) Factors affecting sagittal malalignment due to cage subsidence in standalone cage assisted anterior cervical fusion. Eur Spine J 16:1395–1400. https://doi.org/10.1007/s00586-006-0284-8
25. Purushothaman YMS, Humm J, Jebaseelan D, Yoganandan N (2021) Neck vertebral Level-specific forces and moments under G-x accelerative loading. Mil Med 186:625–631. https://doi.org/10.1093/milmed/usaa338